ENGINEERING RESEARCH JOURNAL (ERJ)
Vol. 1, No. 42 October 2019, pp.1-7.
Journal Homepage: www.feng.bu.edu.eg

Experimental Study on the Performance Enhancement of a Solar Seawater Desalination System*

M.T. Elazab, M.R. Salem, H.A. Refaey, A.A. Abd-Elaziz

Mechanical Engineering Department, Faculty of Engineering at Shoubra, Benha University, 108 Shoubra St., 11629, Cairo, Egypt

Abstract
In this paper, an experimental and theoretical discussion of a humidification and dehumidification (HDH) solar desalination system is presented. The influence of the surface area of spherical plastic balls in humidifier packing is examined at different flow rates of both hot brine and cold water, and the temperature of the cooling water. The results demonstrate that gain output ratio (GOR) and productivity are augmented with increasing the ball packing surface area from 1.09 to 1.4 m^2, and with increasing the flow rates of hot/cold streams. While the cold-water inlet temperature has a negative effect.

Keywords: Solar HDH desalination, Humidifier packing, GOR, Productivity.

1. Introduction

The utmost serious challenge to human kind in the current days is how to fulfill his needs of water [1]. No less than 15-20 L/day of pure water is necessary for basic needs, which are required to be about 50 L/day for each person [2]. In 2030, it is expected that people will need 6900 Bm^3 of pure water, nevertheless, the available now is 4500 Bm^3 [3]. Various desalination techniques were conducted to make the seas and oceans water be valid for drinking and other usage. These technologies like multi-stage flash, vapor compression, etc. are for huge sizes, and are very exaggerate. But humidification and dehumidification system (HDHS) is suitable for small capacities; about 150 kJ/kg of specific energy consumption [4]. The classification of HDHS is according to the energy source, the configuration of air/water cycle and the heating system. The major elements of this HDHS are the evaporator (humidifier), the condenser coils (dehumidifier), the heating system for air/water streams.

Yıldırım and Solmuş [5] inspected theoretically the influence of solar HDHS for various parameters of the system. It was mentioned that the change in cooling water flow rate with cooling water temperature on productivity were significant. Ahmed et al. [6] studied experimentally a corrugated packing. It was observed that the mass and heat transfer processes were augmented. The estimated total cost was about $0.01 for one liter of fresh water. Yuan et al. [7] investigated 1000 L/day solar HDHS. The results showed that water production of the system could reach 1200 L/day, when the average solar radiation raised to about 550 W/m^2. Narayan et al. [8] Discussed theoretically how to perform maximum GOR for air and water heated cycle. Kabeel et al. [9] practically operated HDHS. The optimal ratio of cold/hot water temperature was obtained. The experiments showed that the maximum productivity was obtained when cold-water to hot water temperature ratio was twice. Sharqawy et al. [10] demonstrated that higher GOR could be accomplished by employing large-scale HDHS. Furthermore, increasing the temperature of hot water stream reduces GOR. In the present investigation, a comparison between different surface areas of a plastic ball packing inside the bed humidifier is conducted. This will be considered at wide range of operating conditions; hot/cold water, air mass flow rates, to optimize the performances of HDHS.

2. Experimental setup

These experiments are accomplished in August and September 2018 from 9 A.M. to 3 P.M. The outline of this optimized HDHS is represented in Fig. 1. The main parts include a humidifier, dehumidifier, air and water heating systems. The air heating system uses air solar collector and blower. The heating saltwater system uses parabolic trough and evacuated tube solar collector, tanks, electrical heater, pump, pressure gauges, valves, TDS meter, cooling unit and pyrometer. The desalinate water system uses HDHS, humidity measuring device, packing fill material for the HDH, water spray, cooling water coil, selector switch. For the temperature measuring, thermocouples, temperature gun, digital thermometer and thermostat are utilized.

The blower circulates the air into the cycle, but before the air entering the cycle, it flows in an air solar heater

* Accepted August 20, 2019

and then passes over a water heater before entering the humidifier with a packing filling with different surface areas. In the other inlet basin, the pump starts pumping the water from the tank to spray nozzles inside the humidifier passing over an evacuated tube and an electrical heater. Now the hot water of temperature $T_{w,h}$ and the air of temperature $T_{a,i}$ interface with a liquid to gas ratio at the mass and heat exchanger packing device with a highly specific contact area. The air carries the humidified steam and goes to the dehumidifier passing from a connection chamber, the humid air with a high specific humidity and enthalpy will condensing into the dehumidifier on the cooling coil that has a cooling temperature $T_{cw,1}$ and flow rate revealed in Fig. 2. The description of hybrid solar system presented in Table 1. The maximum solar intensity is at 1:00 P.M. about 950 w/m^2.

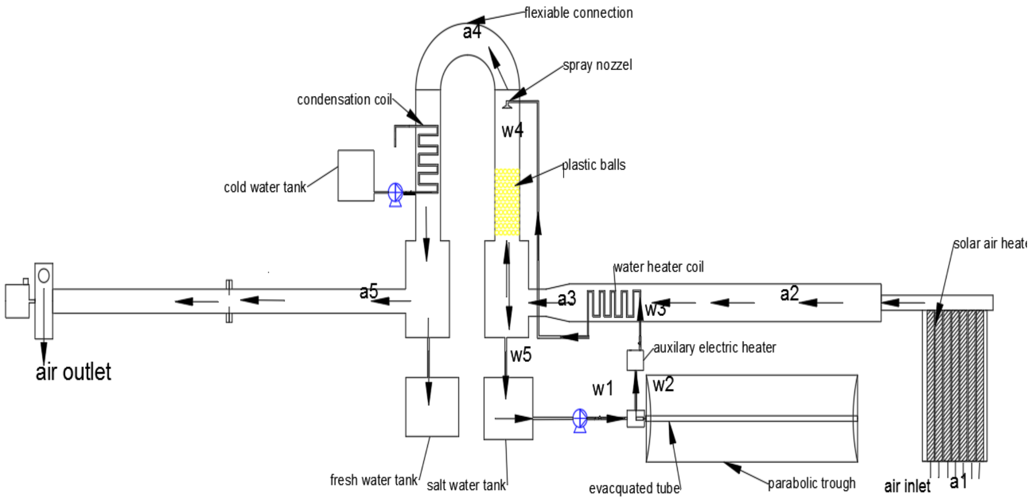

Fig. 1: A diagram of the setup.

Table 1: Specifications of the HDHS.

Technical specifications	**Value**
Humidifier	
Type	Counter flow heat exchanger
Acrylic fibers with thickness, mm	10
Dimensions (length, width, height), cm	21*21*100
Packing dimensions, cm	19*19*70
Spherical plastic ball packing shape (A), m^2	1.4
Spherical plastic ball packing shape (B), m^2	1.09
Dehumidifier	
Type	Counter flow heat exchanger
Acrylic fibers with thickness, mm	10
Dimensions (length, width, height), cm	21*21*100
Cooling coil length, m	6.8
Thickness, inch	3/8
Air solar collector	
Dimensions (length, width, thickness), cm	100*55*15
Insulation thickness, cm	5
Thermal conductivity, W/m.K	0.045
Solar collector angle, Degree	45°
Steel frame carrier	
Main duct	
Shape	Rectangular
Dimensions, cm	35*35*300
Material	Galvanized steel
Thickness, mm	3
Air heating coil	
Length, m	7.5
Diameter, inch	3/8
Pitch, cm	7
Glass wall insulation	
Highest usage temperature, °C	410
Thickness, mm	25

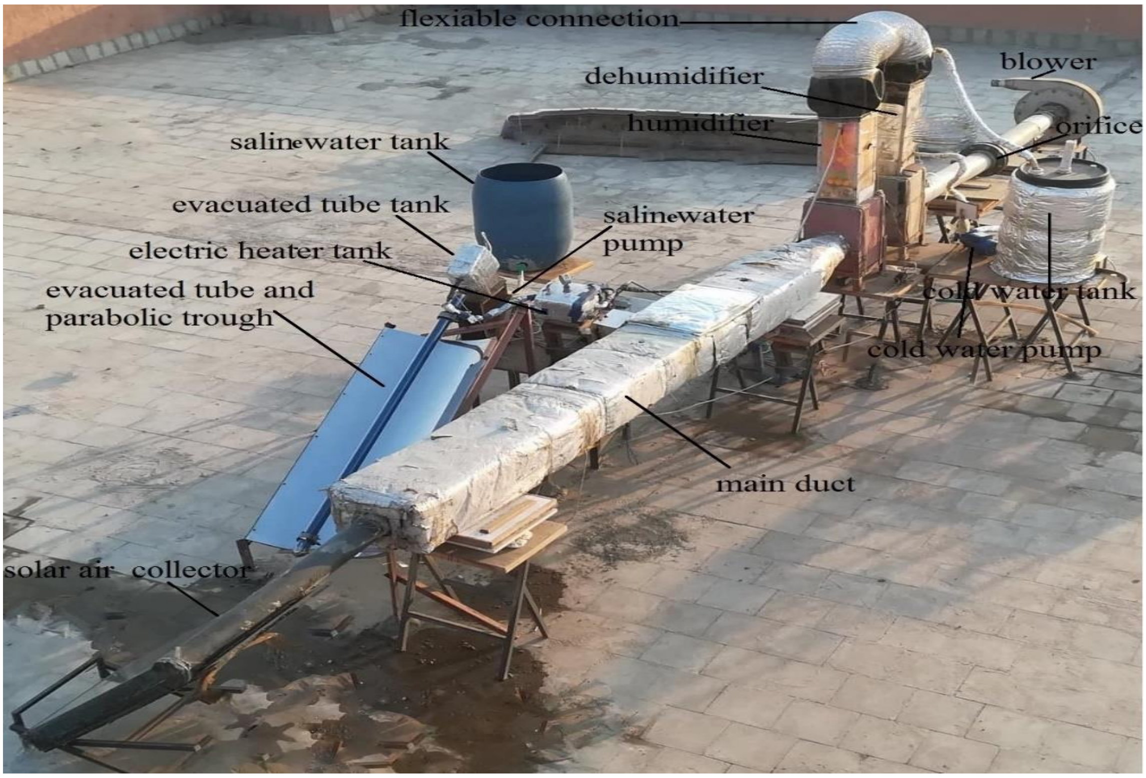

Fig. 2: Photograph of the experimental setup.

Fig. 3 represents a 2D drawing for plastic ball packing used in this work as a packing fill material, the packing with higher surface area works as a mass and heat transfer exchanger device better than other packing with lower surface area. All the temperatures of the hot and cold-water streams entering and leaving the system, the dry/wet bulb temperatures on the air stream inside this cycle, the flow rate of the air and water into the humidifier, the flow rate of the cooling water into the coil. T-type thermocouples with 0.2 mm diameter are used to measure the wet/dry bulb temperatures for all point on the system. A digital reader with resolution of ±0.5℃ is incorporated to display the thermocouples outputs throughout a selector switch [11].

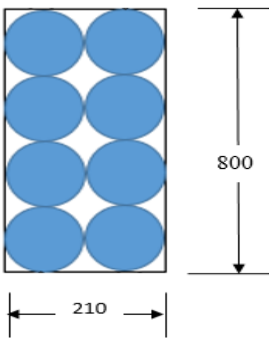

Fig. 3: Diagram for plastic fill packing spheres (dimensions in mm).

3. Theoretical thermal analysis

Energy balance for evacuated tube (water inlet)

$$Q_{sun} = E * A = \dot{m}_w * Cp_w * (T_{w2} - T_{w1}) \quad (1)$$

The power of the electrical water heater

$$Q = E * A = \dot{m}_w * Cp_w * (T_{w3} - T_{w2}) \quad (2)$$

Energy balance for the air solar heater

$$Q_{gain} = Q_{in} - Q_{out} = \dot{m}_a * Cp_a * (T_{a2} - T_{a1}) \quad (3)$$

Energy balance for water-air heater exchanger; for the convection thermal resistance at air side ($R_{conv,a}$):

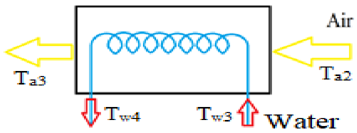

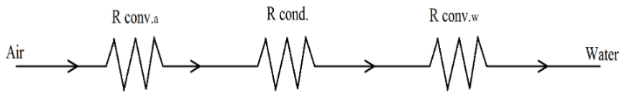

$$R_{conv,a} = \frac{1}{h_{conv,a} * A_o} = \frac{1}{h_{conv,a} * 2\pi * r_o * L_{pipe}} = \frac{1}{2.4315 * 2\pi * 0.00635 * 7.5} \quad (4)$$

For the convection thermal resistance at water side ($R_{conv,w}$):

$$R_{conv,w} = \frac{1}{h_{conv,w} * A_i} = \frac{1}{h_{conv,w} * 2\pi r_i L_{pipe}} \quad (5)$$

$$R = R_{conv,a} + R_{conv,w} \quad (6)$$

$$Q = \dot{m}_a * Cp_a * (T_{a3} - T_{a2}) = \dot{m}_w * Cp_w * (T_{w3} - T_{w4}) = \frac{\Delta T_{lm}}{R} \quad (7)$$

$$\Delta T_{lm} = \frac{\Delta T_1 - \Delta T_2}{\ln\left(\frac{\Delta T_1}{\Delta T_2}\right)} = \frac{(T_{w3} - T_{a2}) - (T_{w4} - T_{a3})}{\ln\left[\frac{(T_{w3} - T_{a2})}{(T_{w4} - T_{a3})}\right]} \quad (8)$$

Energy balance for the humidifier

$$Q = \dot{m}_a * Cp_a * (T_{a4} - T_{a3}) \quad (9)$$

$$Q = \dot{m}_w * Cp_w * (T_{w4} - T_{w5}) \quad (10)$$

Energy balance for the dehumidifier

$$Q = \dot{m}_a * Cp_a * (T_{a4} - T_{a5}) = \dot{m}_w * Cp_w * \left(T_{cw,o} - T_{cw,i}\right) = \frac{\Delta T_{lm}}{R} \quad (11)$$

The specific heat values are available in Table 2 & h_{fg} = 2,335,000 J/kg.

Table 2: Variables values for mathematical calculations [12].

Item	Cp(J/kg.K)	Absorptivity	Emissivity
Hot saline water	4180	0.050	0.960
Ambient Air	1005	-	-

4. Experimental procedures

Firstly, the following parts are assembled to initiate the experiments: Parabolic trough fitted with evacuated tube and tank (solar water heater), air solar collector, electric heater fitted with tank, water-air heat exchanger, water spray system, humidifier, dehumidifier, air duct, blower, two pumps, pressure gauges, thermocouples and some temperature sensors. The first step is to drive pump to deliver the saline water to evacuated tube tank, drive blower to move air through system. Evacuated tube heats water which is then delivered to a tank to heat the water to the desired temperature. Electric heater tank outlet supply the saline water to water-air heat exchanger to raise the temperature of air coming from solar air heater then the water is sprayed through the nozzles in the humidifier, after spraying water in the humidifier, a layer of hot water droplets is formed around plastic balls, then hot air from duct carry hot water vapor. Air is then move through flexible connection to dehumidifier to condense some of air moisture on cooling water pass and then the condensate is collected in distillated water vessel. The temperatures in different locations (as shown in Fig. 4) are measured.

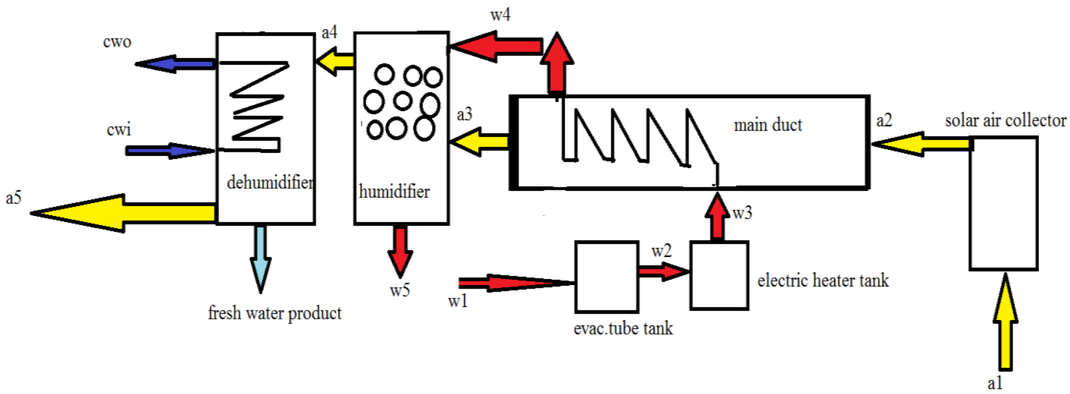

Fig. 4: HDH desalination system layout.

This current system performance can be estimated correctly by express the value of the GOR, the most important parameter [13].

$$\text{GOR} = \frac{\dot{m}_P * h_{fg}}{Q_{in}} \quad (12)$$

5. Results and discussion

In this part, the main target is to find out and compare the effect of the packing filling material and the influences of surface area on the performance of the HDHS. All results on the test rig have been taken from 9 A.M. to 3 P.M. in August and September to guaranteed best solar intensity; the maximum solar intensity was about 900 W/m^2 at 1 P.M. as shown in Fig. 5.

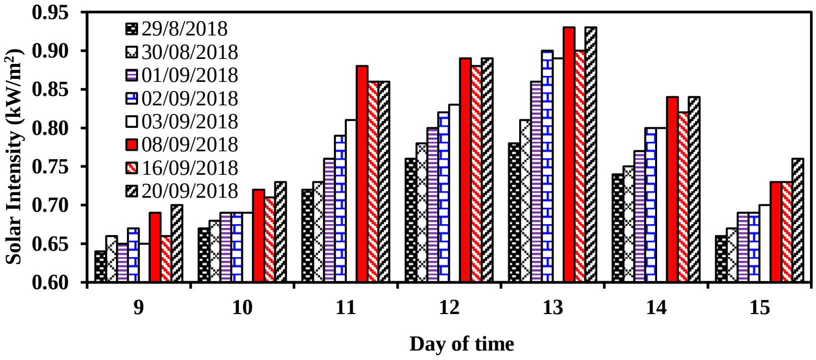

Fig. 5: Solar radiation intensity from 9 A.M. to 3 P.M.

Fig. 6 shows the effect of the contact surface area of the packing plastic balls on the GOR; the packing area is varied from 1.09 to 1.4 m^2. It is denoted that GOR is increased with increasing the contact area. The most important reason is the large contact area between hot water and inlet air entering humidifier that works as a good mass and heat transfer heat exchanger device.

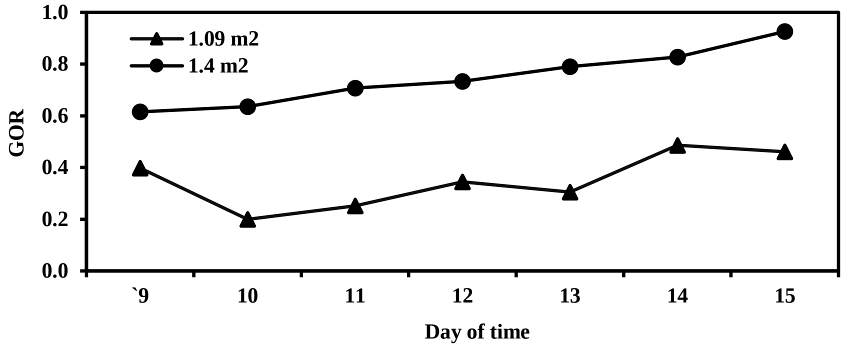

Fig. 6: Effect of contact surface area of packing on GOR.

Fig. 7 signifies the influence of the cold-water temperature in the cooling coil inside the dehumidifier on the HDHS productivity. The results confirm that a significant increasing in the productivity with reducing the cold-water temperature. This is related to dew point temperature; decreasing this inlet water temperature makes the condensation process faster and gives higher production. Fig. 8 shows that an increasing in the HDHS productivity is revealed with increasing the hot saline water flow rate for both packing. But the influence is higher in the plastic packing of 1.4 m^2 than the other packing. This happens because the amount of evaporated liquid increases with increasing the packing area.

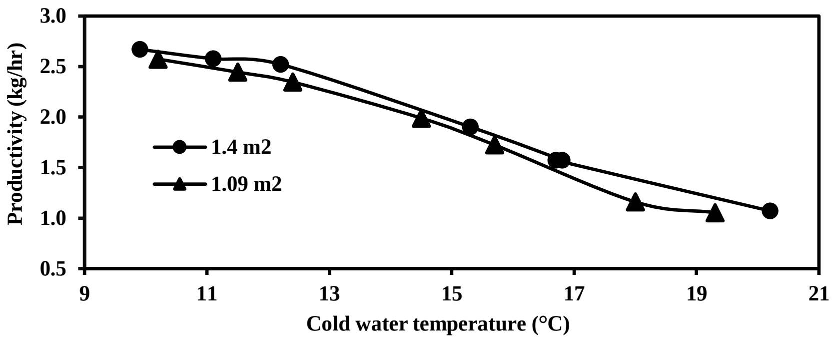

Fig. 7: Effect of cold-water temperature on productivity.

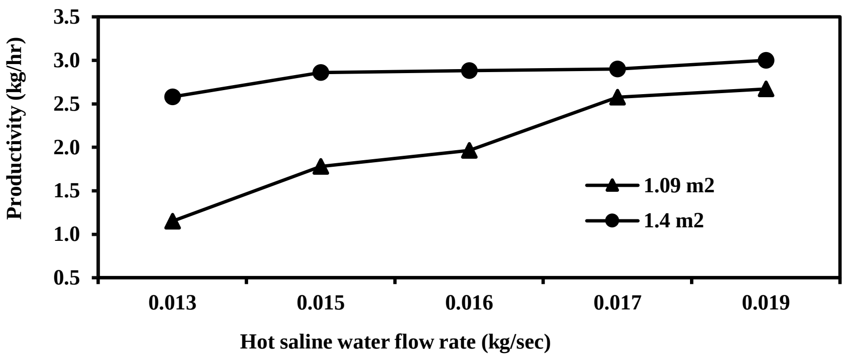

Fig. 8: Effect of hot saline water flow rate on productivity.

Fig. 9 demonstrates the effect of increasing the cold-water flow rate on the HDHS performance. The experiments represent that increasing the cold-water flow rate augments the GOR besides the productivity. This happens because the rate of heat lost increases due to increasing the cold-water flow rate which results in better condensation. Fig. 10 shows an increasing in the moisture flow rate with increasing the packing surface area, which works as an effective mass and heat exchanger device.

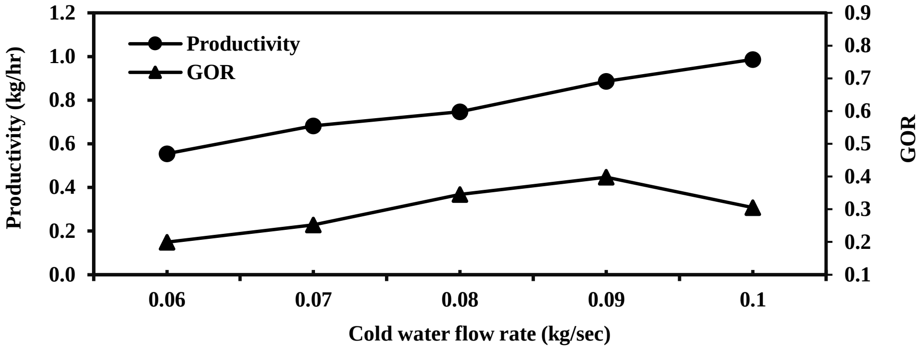

Fig. 9: Effect of cold-water flow rate on productivity and GOR

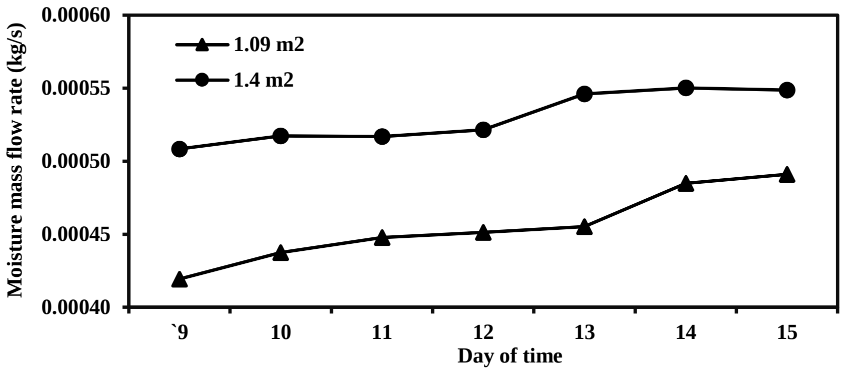

Fig. 10: Effect of packing area on moisture flow rate.

6. Conclusions

According to the experimental results, the following conclusions can be expressed:

- By raising the hot saline water flow rate entering the humidifier and the cold water entering the cooling coil, there is an increase in the HDHS productivity.
- By reducing the cold-water temperature, there is a significant increase in the HDHS productivity.
- The GOR increases with increasing the contact area of the packing material inside the humidifier.
- A plastic ball packing with surface area 1.4 m^2 gives more freshwater production during the day compared to that of area of 1.09 m^2.
- A slight effect for the flow rate and temperature of the air entering the humidifier on the HDHS productivity.

Nomenclature

A	Area, m^2
Cp	specific heat, J/kg.K
E	Energy of the evacuated tube, kW/m^2
h	heat transfer coefficient, W/m^2.K
h_{fg}	Latent heat of vaporization, J/kg
GOR	Gain output ratio
k	Thermal conductivity, W/m.K
$\dot{m}$	Mass flow rate, kg/s
Q	Heat transfer rate, KW
T	Temperature, °C
R	Thermal resistance, $°C/W$

Superscripts and subscripts

a	air
lm	Logarithmic mean
w	water
cw	Cooling water
sw	Saline water

References

[1] M. A. Shannon, P. W. Bohn, M. Elimelech, J. G. Georgiadis, B. J. Marin, and A. M. Mayes, “Science and technology for water purification in the coming decades,” vol. 452, no. March, pp. 301–310, 2008.

[2] L. R. Giorgio Micale, *Seawater Desalination Conventional and Renewable Energy Processes*. 2009.

[3] K. Choon, K. Thu, S. Jin, L. Ang, M. Wakil, and A. Bin, “Recent developments in thermally-driven seawater desalination : Energy ef fi ciency improvement by hybridization of the MED and AD cycles,” *DES*, 2014.

[4] J. Uche, L. Serra, L. A. Herrero, A. Valero, J. A. Turdgano, and C. Torres, “Software for the analysis of water and energy systems,” vol. 156, no. May, pp. 367–378, 2003.

[5] C. Yıldırım and İ. Solmuş, “A parametric study on a humidification – dehumidification (HDH) desalination unit powered by solar air and water heaters” , Energy Conversion and Management, vol. 86, pp. 568–575, 2014.

[6] H.A. Ahmed, I. M. Ismail, W. F. Saleh, and M. Ahmed, “Experimental investigation of humidification-dehumidification desalination system with corrugated packing in the humidifier”, Desalination, vol. 410, pp. 19–29, 2017.

[7] G. Yuan, Z. Wang, H. Li, and X. Li, “Experimental study of a solar desalination system based on humidi fication – dehumidification process”, Desalination, vol. 277, pp. 92–98, 2011.

[8] G. P. Narayan, M. H. Sharqawy, E. K. Summers, J. H. Lienhard, S. M. Zubair, and M. A. Antar, “The potential of solar-driven humidification –

dehumidification desalination for small-scale decentralized water production," *Renew. Sustain. Energy Rev.*, vol. 14, no. 4, pp. 1187–1201, 2010.

[9] A. E. Kabeel, M. H. Hamed, Z. M. Omara, and S. W. Sharshir, "Experimental study of a humidification-dehumidification solar technique by natural and forced air circulation,", Energy, vol. 68, pp. 218-228, 2014.

[10] M. H. Sharqawy, M. A. Antar, S. M. Zubair, and A. M. Elbashir, "Optimum thermal design of humidification dehumidification desalination systems," *Desalination*, vol. 349, pp. 10–21, 2014.

[11] H. M. Factor and G. Grossman, "A packed bed dehumidifier/regenerator for solar air conditioning with liquid desiccants," Solar Energy, vol. 24, no. 6, pp. 541-550, 1980.

[12] Z. M. Omara, A. E. Kabeel, and M. M. Younes, "Enhancing the stepped solar still performance using internal reflectors," *Desalination*, vol. 314, pp. 67–72, 2013.

[13] M. H. Hamed, A. E. Kabeel, Z. M. Omara, and S. W. Sharshir, "Mathematical and experimental investigation of a solar humidification – dehumidification desalination unit," Desalination, vol. 358, pp. 9–17, 2015.